International Journal of Applied Engineering Research ISSN 0973-4562 Volume 13, Number 18 (2018) pp. 13989-14002

Effect of Variable Viscosity and Thermal Conductivity on Heat and Mass Transfer Flow of Nanofluid over a Vertical Cone with Chemical Reaction

S.R. Ravi Chandra Babu[1], *, S. Venkateswarlu[2] and K. Jaya Lakshmi[3]

*[1],*Research scholar, Dept of Mathematics, JNTUA, Anantapur, Andhra Pradesh, India.*

[2]Department of mathematics, RGM College of Engineering & Technology, Nandyal, Andhra Pradesh, India.

[3]Department of mathematics, JNTU College of Engineering Anantapur, Anantapur, Andhra Pradesh, India.

**Corresponding author*

Abstract

We have analyzed the impact of variable properties on heat and mass transfer over a vertical cone filled with nanofluid saturated porous medium with thermal radiation and chemical reaction. Further, the viscosity and thermal conductivity are considered as the function of nanoparticle volume fraction (ϕ). The governing equations represent velocity, temperature and volume fraction of nanoparticles are transformed into the set of ordinary differential equations with similarity variables. These equations together with associated boundary conditions are solved numerically by using an optimized, extensively validated, variational Finite element method. Effects of different parameters such as magnetic parameter (0.5 – 2.5), variable viscosity parameter (2.0 - 200), variable thermal conductivity parameter (0.1 – 2.0), radiation parameter (0.1 – 1.0), thermophoresis parameter (0.1 – 0.5), Brownian motion parameter (0.5 – 2.0), Lewis number (2.0 – 4.0), chemical reaction parameter (0.01 – 0.4) and Suction parameter (1.0 – 4.0) on velocity, temperature and concentration profiles are examined and the results are presented in graphical from. Furthermore, the skin-friction coefficient, Nusselt number and Sherwood number are also investigated and are shown in tabular form.

Keywords: Nanofluid; Vertical cone; Variable viscosity; Variable thermal conductivity; Chemical reaction; Thermal radiation.

NOMENCLATURE:

k_m	Thermal conductivity	Nu_x	Nusselt number
ϕ	Nanoparticle volume fraction	ϕ_w	Nanoparticle volume fraction on the plate
ϕ_∞	Ambient nanoparticle volume fraction	(x, y)	Cartesian coordinates
T_w	Temperature at the plate	T_∞	Ambient temperature attained
T	Temperature on the plate	Ra_x	Rayleigh number
q_w	Wall heat flux	J_w	Wall mass flux
D_B	Brownian diffusion	D_T	Thermophoretic diffusion coefficient
β_0	Strength of magnetic field	g	Gravitational acceleration vector
Nt	Thermophoresis parameter	Le	Lewis number
P	Pressure	Nb	Brownian motion parameter
q_r	Thermal radiation	M	Magnetic parameter
Sh_x	Local Sherwood number	Nv	Variable viscosity parameter
Nc	Variable thermal conductivity parameter	Cr	Chemical reaction parameter
Nr	Buoyancy ratio	K	Permeability of the porous medium

Greek symbols

μ	viscosity	ε	porosity
γ	proportionality constant	α_m	Thermal diffusivity .
ρ_f	Fluid density	ρ_p	Nanoparticle mass density
ψ	Stream function	V	Kinematic viscosity of the fluid
τ	Parameter defined by $\varepsilon \frac{(\rho c)_p}{(\rho c)_f}$	$(\rho c)_f$	Heat capacity of the fluid
∅ (η)	Dimensionless nanoparticle volume fraction	η	Similarity variable
θ (η	Dimensionless temperature	$(\rho c)_p$	Effective heat capacity of the nanoparticle
α	Acute angle of the plate to the vertical	β	Volumetric expansion coefficient

Subscripts

w	Condition on the plate	∞	Condition far away from the plate
η	Similarity variable	f	Base fluid

INTRODUCTION

In recent years the field of nanotechnology has become more popular because of its specific application to the arenas of electronics, fuel cells, space, fuels, better air quality, batteries, solar cells, medicine, cleaner water, chemical sensors and sporting goods. Nanoparticles are the particles and are of 1-100 nm in size. The convectional heat transfer fluids like water, oil, kerosene and ethylene glycol have poor heat transfer capabilities due to their low thermal conductivity. To improve the thermal conductivity of these fluids nano/micro-sized materials are suspended in liquids. Due to the nanofluid thermal enhancement, performance, applications and benefits in several important arenas, the nanofluid has contributed significantly well in the field of microfluidics,manufacturing,microelectronics, advanced nuclear systems, polymer technology, transportation, medical, saving in energy. At the time of doing research on new coolants and cooling technologies, Choi [1] was the first introduced a new type of fluid called nanofluid. Eastman et al. [2] have noticed in an experiment that the thermal conductivity of the base fluid (water) has increased up to 60% when CuO nanoparticles of volume fraction 5% are added to the base fluid. This is because of increasing surface area of the base fluid duo to the suspension of nanoparticles. Eastman et al. [3] have also showed that the thermal conductivity has increased 40% when copper nanoparticles of volume fraction less than 1% are added to the ethylene glycol or oil. Choi et al. [4] have reported that there is 150% enhancement in thermal conductivity when carbon nanotubes are added to the ethylene glycol or oil. Buongiorno [5] has reported seven possible mechanisms associating convection of nanofluids through moment of nanoparticles in the base fluid using scale analysis. Kuznetsov and Nield [6] studied the influence of Brownian motion and thermophoresis on natural convection boundary layer flow of a nanofluid past a vertical plate. Chamkha et al. [7] have analyzed the impact of Soret and Dufour effects on mixed convection flow of nanofluid over a vertical cone saturated in a porous medium with chemical reaction. Gorla et al. [8] have studied nanofluid natural convection boundary layer flow through porous medium over a vertical cone. Behseresht et al. [9] have discussed heat and mass transfer characteristics of a nanofluid over a vertical cone using practical range of thermo-physical properties of nanofluids. Recently, Ghalambaz et al. [10] have analyzed the influence of nanoparticle diameter and concentration on natural convection heat and mass transfer of Al_2O_3 -water based nanofluids over a vertical cone. Noghrehabadi et al. [11, 12, 13] have analyzed the natural convection of nanofluids over a stretching sheet by taking partial slip boundary conditions and prescribed constant wall temperature, vertical plate by taking heat generation/absorption and partial slip respectively. Teamah et al. [14] have presented augmentation of MHD natural convection heat transfer in square cavity by utilizing nanofluids by taking heat source into the account. Sudarsana Reddy et al. [15] have presented natural convection boundary layer heat and mass transfer characteristics of Al_2O_3 - water and Ag - water nanofluids over a vertical cone. Sheremet et al. [16] presented Buongiorno's mathematical model of nanofluid over a square cavity through porous medium. Sheremet et al. [17] have deliberated natural convection heat transfer enhancement of Buongiorno's mathematical model of nanofluid over a porous enclosure. Ellahi et al. [18] have reported Non-Newtonian flow, heat transfer between two coaxial cylinders through nanofluid saturated porous medium with variable viscosity. Sheikholeslami et al. [19] have analyzed the natural convection heat transfer in an elliptic inner cylinder filled with nanofluid.

It is well known fact that the fluid characteristics may varies with temperature, so, to predict exactly the flow, heat and mass transfer characteristics of the fluid it is necessary to consider the viscosity and thermal conductivity of the fluid as the function of temperature [20, 21]. The study of existing literature on nanofluids discloses that the viscosity as well as thermal conductivity of the nanofluid is considered variable properties and are strongly varies with volume fraction of nanoparticles rather than temperature [22, 23]. Khanafer and Vafai [24] have conducted both experimental and theoretical reviews to analyze the thermo physical properties of the nanofluids. Kakac and Pramuanjaroenkij [25] have also examined the thermo physical features of nanofluids. They [24, 25] concluded that the dynamic viscosity and thermal conductivity of the nanofluids are strongly depending on concentration of nanoparticles. Noghrehabadi et al. [26] reported the natural convection boundary layer flow and heat transfer analysis over a vertical cone embedded in porous medium saturated with nanofluid. Sudarsana Reddy et al. [27] have discussed the effect of variable viscosity and thermal conductivity on heat and mass transfer flow of nanofluid over a stretching sheet.

The main aim of this article is to address the influence of variable viscosity and variable thermal conductivity on MHD boundary layer heat and mass transfer flow of nanofluid over a vertical cone embedded in porous medium with thermal radiation and chemical reaction. In this analysis the viscosity and thermal conductivity are considered as the functions of local concentration of nanoparticles. As a result, variable viscosity and thermal conductivity parameters are entered into the problem. The problem presented here has immediate applications in biomedical systems, electronic devices, food processing, manufacturing, cooling systems, etc. To our knowledge, the problem is new and no such articles reported yet in the literature.

MATHEMATICAL ANALYSIS OF THE PROBLEM

Fig. 1 demonstrates a steady two-dimensional viscous incompressible nanofluid flow over a vertical cone embedded in porous medium in the presence of variable viscosity and thermal conductivity. A magnetic field of strength B_0 applied in the direction normal to the surface of the cone. It is assumed that the temperature and nanoparticle volume fraction at the surface of the cone (y=0) are T_w, and ϕ_w and the temperature and nanoparticle volume fraction of the ambient fluid are T_∞ and ϕ_∞, respectively. By employing the Oberbeck - Boussinesq approximation the governing equations describing the steady-state conservation of mass, momentum, energy as well as conservation of nanoparticles for nanofluids in the presence of thermal radiation and chemical reaction parameters take the following form:

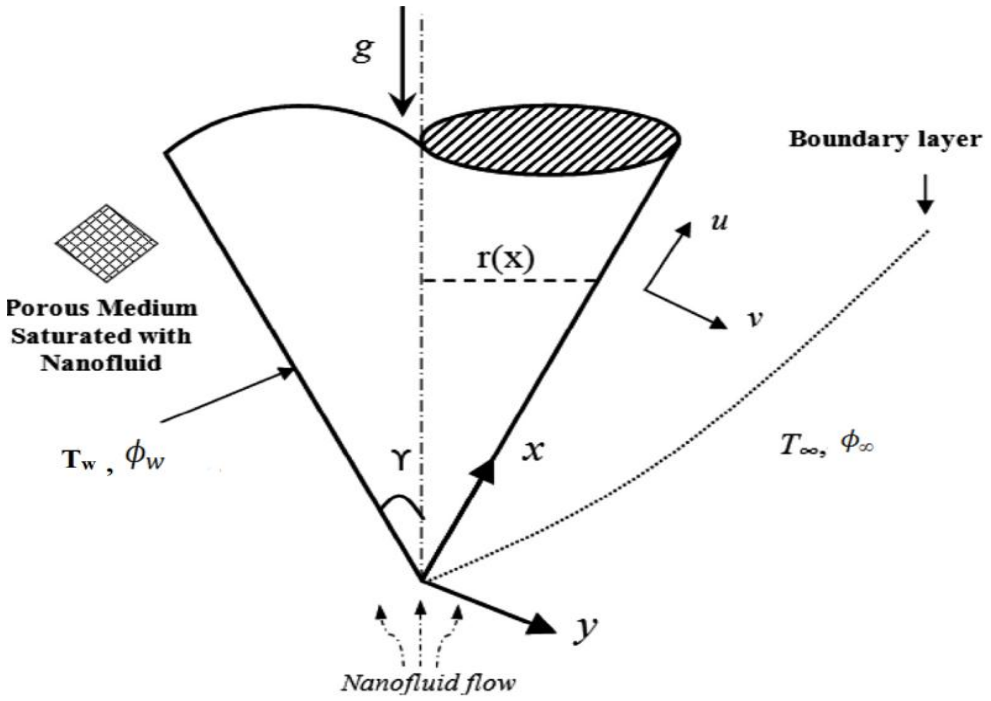

Figure 1. Physical model and coordinate system

$$\frac{\partial(ru)}{\partial x}+\frac{\partial(rv)}{\partial y}=0 \tag{1}$$

$$\frac{\partial p}{\partial y}=0 \tag{2}$$

$$\frac{\partial p}{\partial x}=-\frac{\mu(\phi)}{K}u+g\,[(1-\phi_\infty)\rho_{f\infty}\beta(T-T_\infty)-(\rho_p-\rho_{f\infty})(\phi-\phi_\infty)]\cos\gamma-\frac{\sigma\beta_0^2}{\rho_f}u \tag{3}$$

$$\left(u\frac{\partial T}{\partial x}+v\frac{\partial T}{\partial y}\right)=\frac{1}{(\rho c_p)_{nf}}\frac{\partial}{\partial y}\left(k_m(\phi)\frac{\partial T}{\partial y}\right)+\frac{(\rho c)_p}{(\rho c_p)_{nf}}\left[D_B\frac{\partial\phi}{\partial y}.\frac{\partial T}{\partial y}+\left(\frac{D_T}{T_\infty}\right)\left(\frac{\partial T}{\partial y}\right)^2\right]-\frac{1}{(\rho c_p)_{nf}}.\frac{\partial}{\partial y}(q_r) \tag{4}$$

$$\frac{1}{\varepsilon}\left(u\frac{\partial\phi}{\partial x}+v\frac{\partial\phi}{\partial y}\right)=D_B\frac{\partial^2\phi}{\partial y^2}+\left(\frac{D_T}{T_\infty}\right)\frac{\partial^2 T}{\partial y^2}-K_r(\phi-\phi_\infty) \tag{5}$$

The boundary conditions based on the problem description are as follows:

$$u=0,\ v=V_1(x),\ T=T_w,\qquad \phi=\phi_w\qquad at\quad y=0 \tag{6}$$

$$u\to 0, T\longrightarrow T_\infty,\ \phi\longrightarrow\phi_\infty\quad at\ y\to\infty \tag{7}$$

The term $V_1=-\frac{3}{4}\frac{\alpha}{x}Ra_x^{1/4}V_0$ denotes the surface mass transfer with $V_1<0$ (suction) and $V_1>0$ (injection). It is similar to $V_0>0$ represents to suction and $V_0<0$ represents to injection.

In the present study, the viscosity and thermal conductivity are taken as the reciprocal and a linear function of nanoparticle volume fraction, respectively. Therefore, the viscosity in terms of nanoparticle volume fraction can be written as follows:

$$\frac{1}{\mu}=\frac{1}{\mu_\infty}[1+\gamma(\phi-\phi_\infty)] \tag{8}$$

The above equation can be simplified as

$$\frac{1}{\mu}=m_\mu(\phi-\phi_r) \tag{9}$$

Where, m_μ and ϕ_r are can be defined as

$$m_\mu=\frac{\gamma}{\mu_\infty}\ \text{and}\quad \phi_r=\phi_\infty-\frac{1}{\gamma}.$$

In the above equations (8) and (9), μ_∞, m_μ, ϕ_∞, ϕ_r, and γ are constant values.

The thermal conductivity as a function of volume fraction of nanoparticle is defined as

$$k_m(\phi)=k_{m,\infty}\left(1+m_k(\phi-\phi_\infty)\right) \tag{10}$$

Where, $m_k=\frac{Nc}{(\phi_w-\phi_\infty)}$ and *Nc* is the variable thermal conductivity parameter, $k_{m,\infty}$ is the effective thermal conductivity.

By using Rosseland approximation for radiation, the radiative heat flux q_r is defined as

$$q_r = -\frac{4\sigma^*}{3K^*}\frac{\partial T^4}{\partial y} \quad (11)$$

where σ^* is the Stephan-Boltzman constant, K^* is the mean absorption coefficient. We assume that the temperature differences within the flow are such that the term T^4 may be expressed as a linear function of temperature. This is accomplished by expanding T^4 in a Taylor series about the free stream temperature T_∞ as follows:

$$T^4 = {T_\infty}^4 + 4{T_\infty}^3(T - T_\infty) + 6{T_\infty}^2(T - T_\infty)^2 + \cdots \quad (12)$$

Neglecting higher-order terms in the above equation (12) beyond the first degree in $(T - T_\infty)$, we get

$$T^4 \cong 4{T_\infty}^3 T - 3{T_\infty}^4 . \quad (13)$$

Thus, substituting Eq. (13) into Eq. (11), we get

$$q_r = -\frac{16{T_\infty}^3\sigma^*}{3K^*}\frac{\partial T}{\partial y}. \quad (14)$$

The continuity equation (1) is satisfied by introducing a stream function (ψ) as

$$u = \frac{1}{r}\frac{\partial \psi}{\partial y}, \qquad v = -\frac{1}{r}\frac{\partial \psi}{\partial x} \quad (15)$$

The following similarity transformations are introduced to simplify the mathematical analysis of the problem

$$\eta = \frac{y}{x}Ra_x^{1/2}, \quad f(\eta) = \frac{\psi}{\alpha_m . r . Ra_x^{1/2}}, \quad \theta(\eta) = \frac{T - T_\infty}{T_w - T_\infty},$$

$$\emptyset(\eta) = \frac{\phi - \phi_\infty}{\phi_w - \phi_\infty}, \quad Nv = \frac{\phi_r - \phi_\infty}{\phi_w - \phi_\infty} \quad (16)$$

Where Ra_x is the local Rayleigh number and is defined as

$$Ra_x = \frac{g\beta K\rho_{f\infty}(1 - \phi_\infty)(T_w - T_\infty)\, x\, Cos\gamma}{\mu_\infty \alpha_m} \quad (17)$$

and ' r ' can be approximated by the local radius of the cone, if the thermal boundary layer is thin, and is related to the x coordinate by $r = x\, sin\gamma$.

Using the similarity variables (16) and making use of Eqn. (14), the governing equations (3) - (5) together with boundary conditions (6) and (7) reduce to

$$Nv(Nv - \emptyset)f'' + Nv\, f'\emptyset' - (Nv - \emptyset)^2(\theta' - Nr\, \emptyset') - (Nv - \emptyset)^2 M f' = 0 \quad (18)$$

$$(1 + R)\theta'' + Nc\, \emptyset\, \theta'' + \frac{3}{2} f\, \theta' + Nc\, \theta'\emptyset' + Nt(\theta')^2 + Nb\, f'\theta' = 0 \quad (19)$$

$$\emptyset'' + \frac{3}{2} Le\, f\, \emptyset' + \frac{Nt}{Nb}\, \theta'' - Cr\, \emptyset = 0 \quad (20)$$

The transformed boundary conditions are

$$\eta = 0, \ f = V_0 \ \ f' = 0, \ \theta = 1, \emptyset = 1.$$
$$\eta \longrightarrow \infty, \ f' = 0, \ \theta = 0, \ \emptyset = 0. \quad (21)$$

where prime denotes differentiation with respect to η, and the key,thermophysical parameters dictating the flow dynamics are defined by

$$Nr = \frac{(\rho_p - \rho_{f\infty})(\phi_w - \phi_\infty)}{\rho_{f\infty}\beta(T_w - T_\infty)(1 - \phi_\infty)}, \ Nb = \frac{\varepsilon\beta(\rho c)_p D_B(\phi_w - \phi_\infty)}{(\rho c)_f\, \alpha_m},$$

$$Nt = \frac{\varepsilon(\rho c)_p D_T(T_w - T_\infty)}{(\rho c)_f\, \alpha_m T_\infty}, \ Le = \frac{\alpha_m}{\varepsilon D_B}, Nv = -\frac{1}{\gamma(\phi_w - \phi_\infty)},$$

$$M = \frac{\sigma {\beta_0}^2 x}{\rho {Ra_x}^{1/2}}, \ R = \frac{16{T_\infty}^3\sigma^*}{3K^* k}, \ Cr = \frac{k_0 x^2}{D_B Ra_x}.$$

Quantities of practical interest in this problem are local Nusselt number Nu_x, and the local Sherwood number Sh_x, which are defined as

$$Nu_x = \frac{x q_w}{k_{m,\infty}(T_w - T_\infty)}, \quad Sh_x = \frac{x J_w}{D_B(\phi_w - \phi_\infty)} \quad (22)$$

Here, q_w is the wall heat flux and J_w is the wall mass flux.

The set of ordinary differential equations (18) – (20) are highly non-linear, and therefore cannot be solved analytically. The Finite-element method [28, 29, 30, 31] has been implemented to solve these non-linear equations.

NUMERICAL METHOD OF SOLUTION

The Finite-element method (FEM) is such a powerful method for solving ordinary differential equations and partial differential equations. The basic idea of this method is dividing the whole domain into smaller elements of finite dimensions called finite elements. This method is such a good numerical method in modern engineering analysis, and it can be applied for solving integral equations including heat transfer, fluid mechanics, chemical processing, electrical systems, and many other fields. The steps involved in the finite-element method are as follows.

(i) Finite-element discretization

(ii) Generation of the element equations

(iii) Assembly of element equations

(iv) Imposition of boundary conditions

(v) Solution of assembled equations

RESULTS AND DISCUSSION

Numerical examination of the boundary value problem (18) – (20) together with boundary conditions (21) has been conducted to deliver the physical incite of the flow problem and the results are shown graphically from Figs. 2 - 22. The results obtained in the present study are compared with the results of Noghrehabadi et al. [26] and are shown in table 1.

The velocity (f'), temperature (θ) and concentration of nanoparticle (∅) profiles with magnetic parameter (M) are depicted in Figs. 2 – 4. The thickness of hydrodynamic boundary layer decelerates, whereas, the thickness of thermal

and solutal boundary layers is heightens with enhance in the values of (*M*). The presence of magnetic field in an electrically conducting fluid produces a force called Lorentz force, this force acts against the flow direction causes the depreciation in velocity profiles (Fig 2), and at the same time, to overcome the drag force imposed by the Lorentzian retardation the fluid has to perform extra work; this supplementary work can be converted into thermal energy which increases the temperature of the fluid (Fig 3) and also increases the concentration profiles (Fig 4).

The impact of different values of variable viscosity parameter (*Nv*) on velocity, temperature and nanoparticle volume fraction profiles are plotted in Figs. 5 – 7. It is clearly noticed from Fig.5 that the velocity profiles are highly influenced by the variable viscosity parameter (*Nv*) in the vicinity of the cone surface. But, in the areas far away from the cone surface, inside the boundary layer, the velocity profiles are poorly affected by (*Nv*). The temperature distributions are decelerated in the boundary layer region (Fig. 6) with the rising values of variable viscosity parameter (*Nv*). It is noted from Fig. 7 that the nanoparticle concentration distributions are deteriorated significantly from the surface of the cone into the boundary layer as the values of (*Nv*) increased.

Figs. 8 and 9 illustrate the effect of variable thermal conductivity parameter (*Nc*) on the dimensionless temperature and concentration profiles in the boundary layer region. An increase in the values of variable thermal conductivity parameter (*Nc*) elevates the magnitude of temperature distributions (Fig. 8). This is because of the fact that the thermal conductivity of the nanofluid raises near the cone surface as the values of variable thermal conductivity parameter (*Nc*) increases. However, the thickness of the solutal boundary layer decelerates near the cone surface with the improving values of (*Nc*).

The non-dimensional profiles of temperature and concentration of nanoparticles are displayed in Figs. 10 and 11 for various values of radiation parameter (*R*). With the higher values of (*R*) the temperature of the fluid rises in the boundary layer regime. This is because of the fact that imposing thermal radiation into the flow warmer the fluid, which causes an increment in the thickness of thermal boundary layer in the entire flow region (Fig.10). However, the concentration boundary layer thickness is deteriorated with increasing values of *R.*

Figures 12 and 13 depict the temperature (θ) and concentration (∅) distributions for various values of thermophoretic parameter (*Nt*). Both the temperature and concentration profiles elevate in the boundary layer region for the higher values of thermophoretic parameter (*Nt*). Because of temperature gradient the thermophoretic force was developed in the boundary layer region and this force involves in the diffusion of nanoparticles from higher temperature region to the lower temperature region, causes the enhancement in the thickness of both thermal and concentration boundary layers.

Figures 14 – 15 shows the influence of Brownian motion parameter (*Nb*) on thermal and solutal boundary layer thickness. Brownian motion is the arbitrary motion of suspended nanoparticles in the base fluid and is more influenced by its fast moving atoms or molecules in the base fluid. It is worth to mention that Brownian motion is related to the size of nanoparticles and are often in the form of agglomerates and/or aggregates. It is noticed that, with the increasing values of Brownian motion parameter (*Nb*) the temperature of the fluid is elevated in the boundary layer regime (Fig.14). However, the concentration profiles are decelerated in the fluid regime as the values of (*Nb*) increases (Fig.15).

The influence of Lewis number (*Le*) on temperature and concentration evolutions is plotted in Figs. 16 and 17. It is observed that both the temperature and concentration distributions decelerate with the increasing values of the Lewis number in the entire boundary layer region. By definition, the Lewis number represents the ratio of thermal diffusivity to the mass diffusivity. Increasing the Lewis number means a higher thermal diffusivity and a lower mass diffusivity, and this produces thinner thermal and concentration boundary layers.

The temperature and concentration profiles are depicted in Figs. 18 – 19 for diverse values of chemical reaction parameter (*Cr*). It is noticed from Fig.18 that the temperature profiles of the fluid decelerated in the entire boundary layer regime with the higher values of chemical reaction parameter (*Cr*). The concentration profiles are highly influenced by the chemical reaction parameter. Chemical reaction parameter (*Cr*) increases means lesser the molecular diffusivity, as the result thinner the solutal boundary layer thickness (Fig.19).

It is perceived from Fig. 20 that the velocity deteriorates with higher values of suction parameter ($V_0 > 0$). The influence of V_0 on temperature distributions for different values of ($V_0 > 0$) is depicted in Fig. 21. This figure indicates that the temperature profiles decelerate with rising values of V_0. We perceived from Fig. 22 that concentration distributions deteriorate with increasing values of V_0.

The values of Skin – friction Coefficient $\left(-f''(0)\right)$ Nusselt number $-\theta'(0)$ and Sherwood number $-\emptyset'(0)$ are calculated for diverse values of the key parameters entered into the problem and the results are shown in Table 2 – 6. It is evident from table 2 that the dimensionless rates of velocity, heat and mass transfer are all decelerates with the increasing values of both magnetic parameter (*M*) and buoyancy ratio parameter (Nr). Table 3 reveals that the magnitude of skin friction coefficient, Nusselt and Sherwood numbers are amplified in the fluid regime as the values of variable viscosity parameter (*Nv*) increases. It is also noticed from this table that the non-dimensional velocity and heat transfer rates depreciate, whereas, non-dimensional mass transfer rates escalate with the higher values of variable thermal conductivity parameter (*Nc*). With rising values of radiation parameter (R) the values of skin – friction coefficient $\left(-f''(0)\right)$ Nusselt number $-\theta'(0)$ and Sherwood number $-\emptyset'(0)$ are all deteriorates as shown in Table 4.

The impact of Brownian motion parameter (*Nb*) and thermophoresis parameter (*Nt*) on skin friction coefficient, Nusselt number and Sherwood numbers is presented

in table 5. Skin – friction coefficient, Nusselt number values decelerate, whereas, Sherwood number values enhances in the fluid region as the values of Brownian motion parameter (*Nb*) rises. It is noticed that the dimensionless rates of velocity, heat and mass transfer are both deteriorates with the higher values of (*Nt*). It is seen from table 6 that Higher the values of Lewis number (Le) and Chemical reaction parameter (*Cr*) intensify the non-dimensionless velocity, heat and mass transfer rates.

GRAPHS :

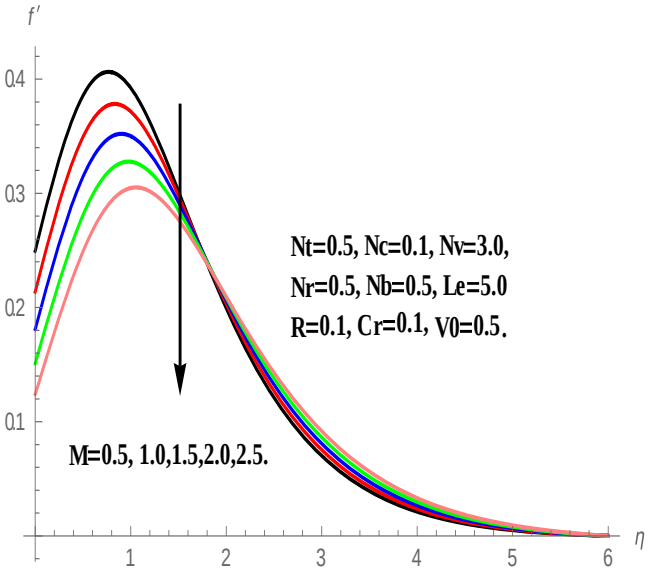

Figure 2.Velocity profiles for various values of (*M*)

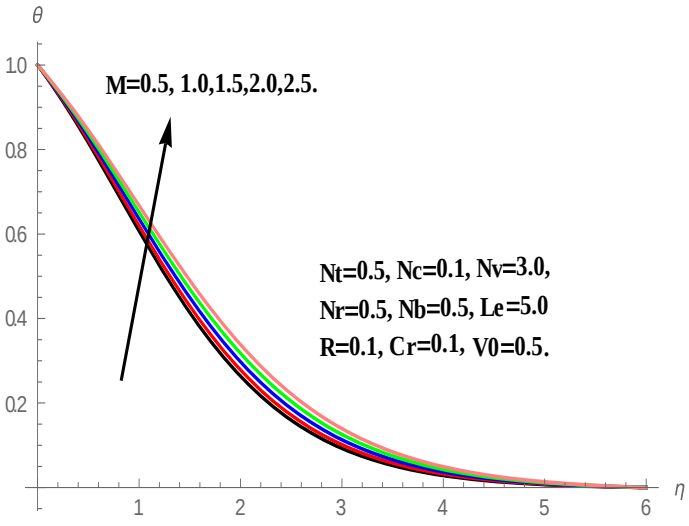

Figure 3.Temperature profiles for various values of (*M*)

.

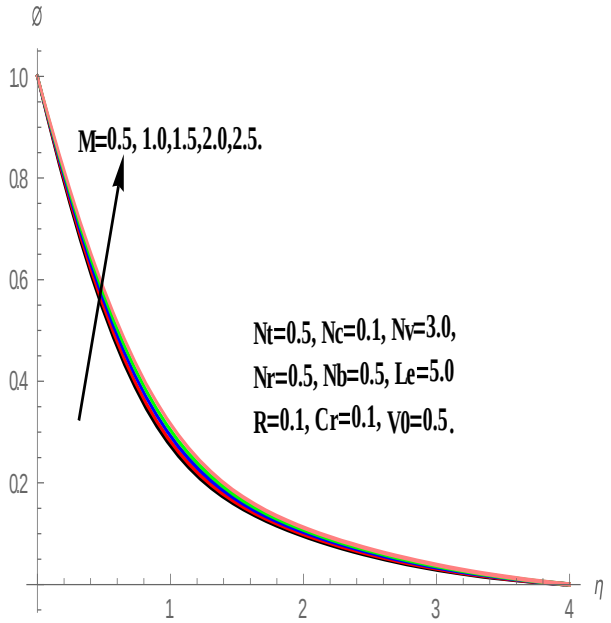

Figure 4.Concentration profiles for various values of (*M*)

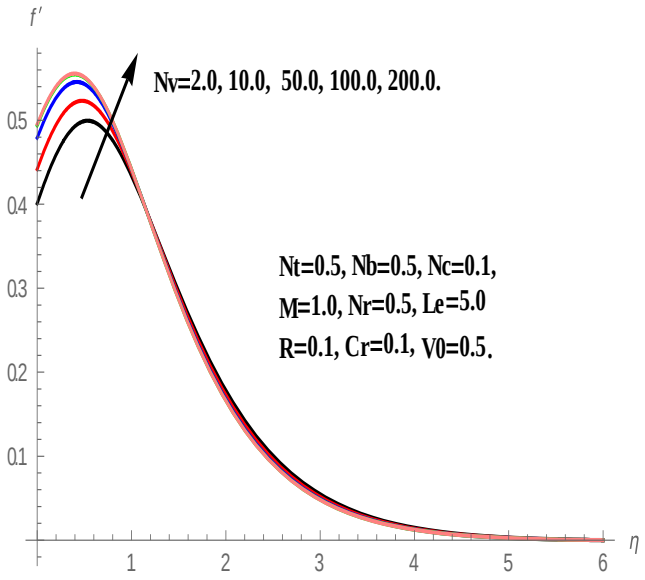

Figure 5.Velocity profiles for various values of (*Nv*)

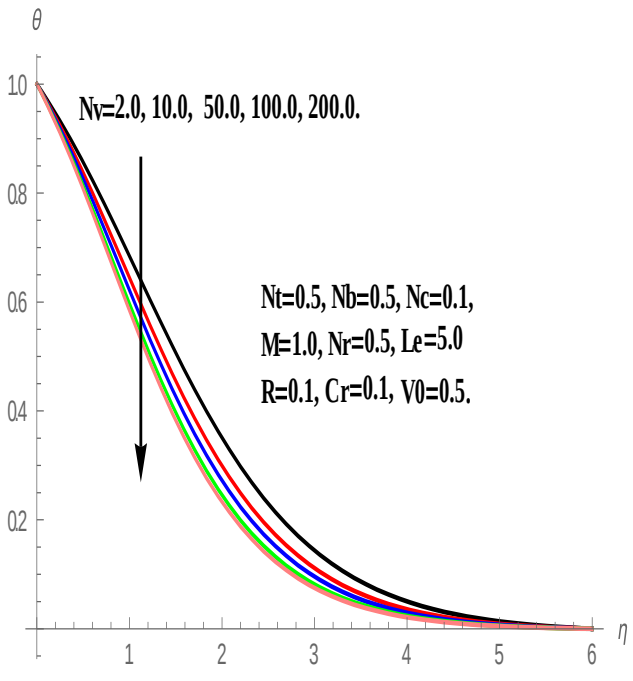

Figure 6.Temperature profiles for various values of (*Nv*)

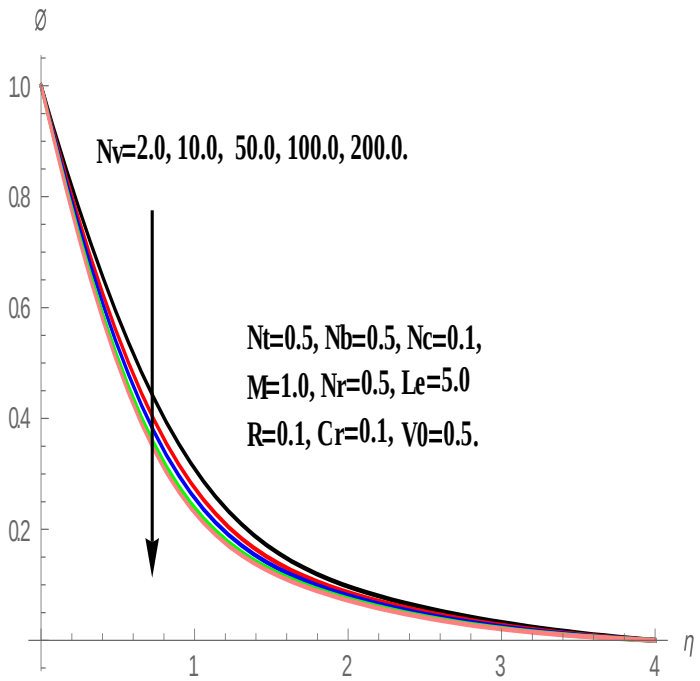

Figure 7.Concentration profiles for various values of (*Nv*)

.

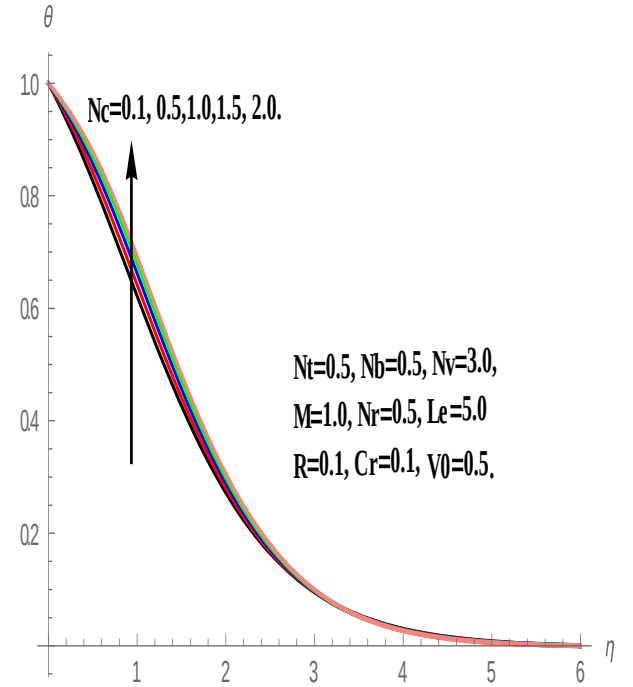

Figure 8.Temperature profiles for various values of (*Nc*)

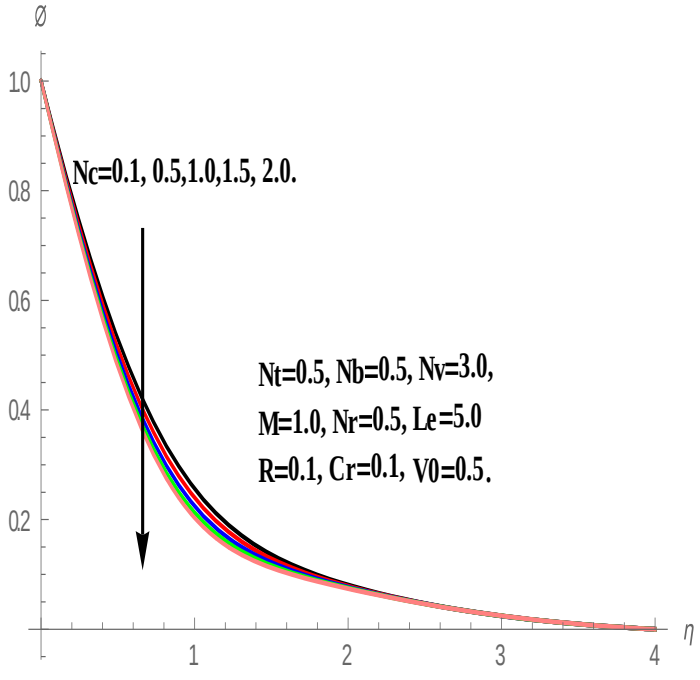

Figure 9.Concentration profiles for various values of (*Nc*)

.

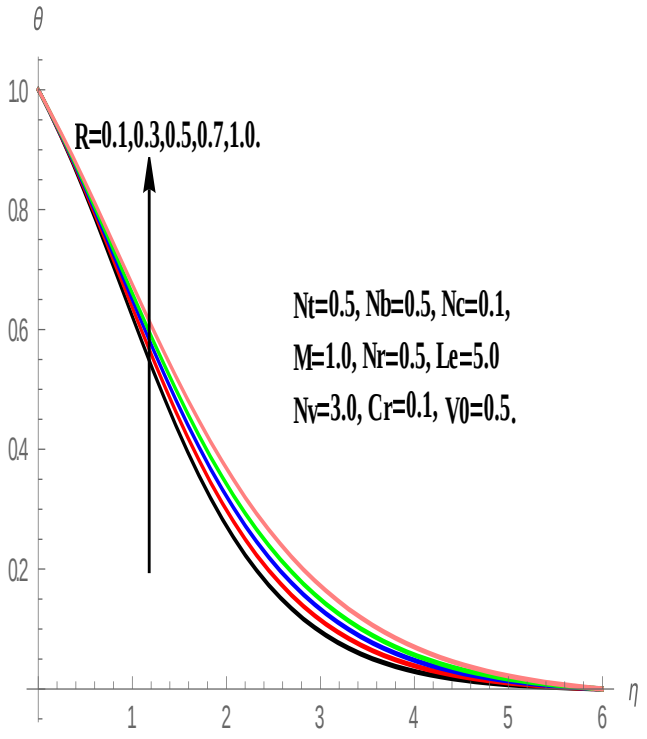

Figure 10.Temperature profiles for various values of (*R*)

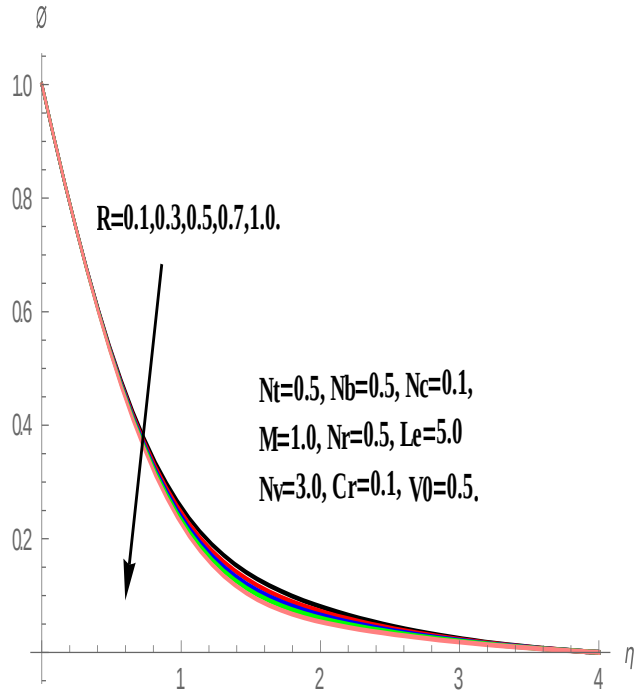

Figure 11.Concentration profiles for various values of (*R*)

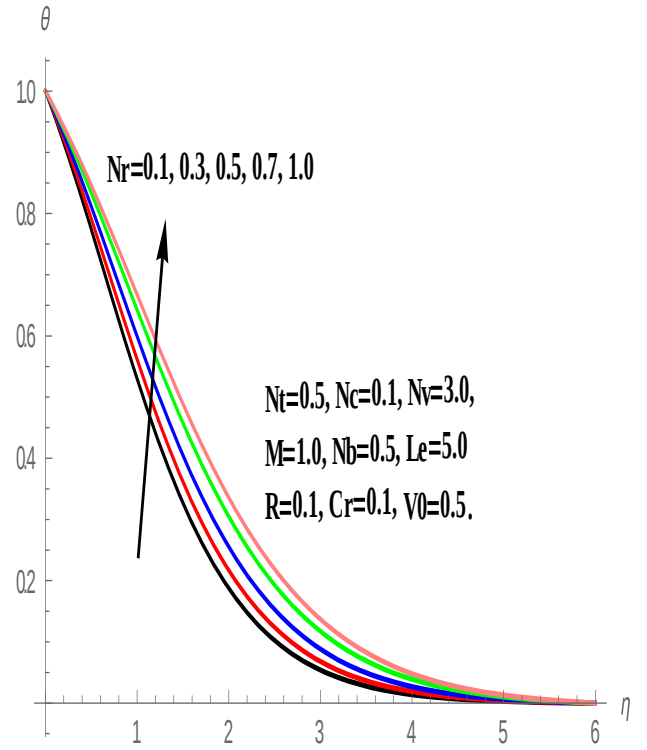

Figure 12.Temperature profiles for various values of (*Nt*)

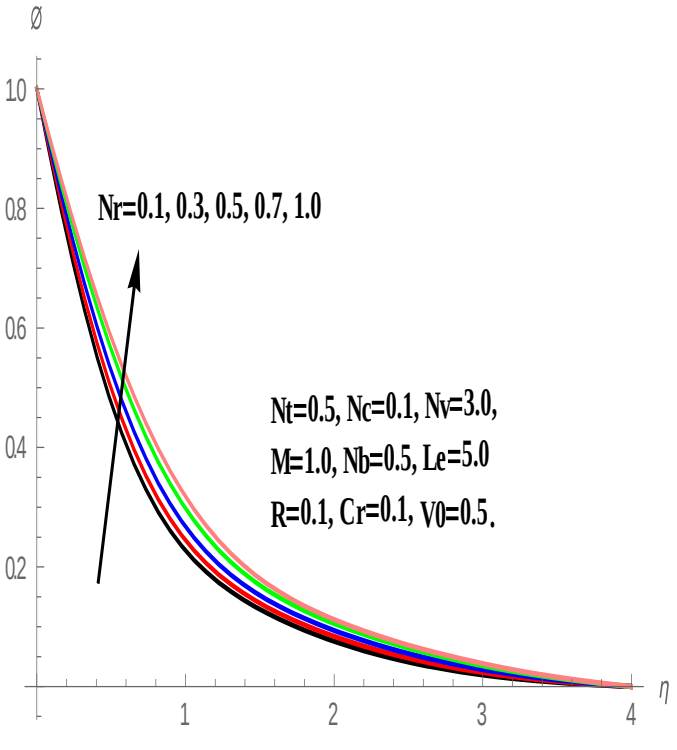

Figure 13.Concentration profiles for various values of (*Nt*)

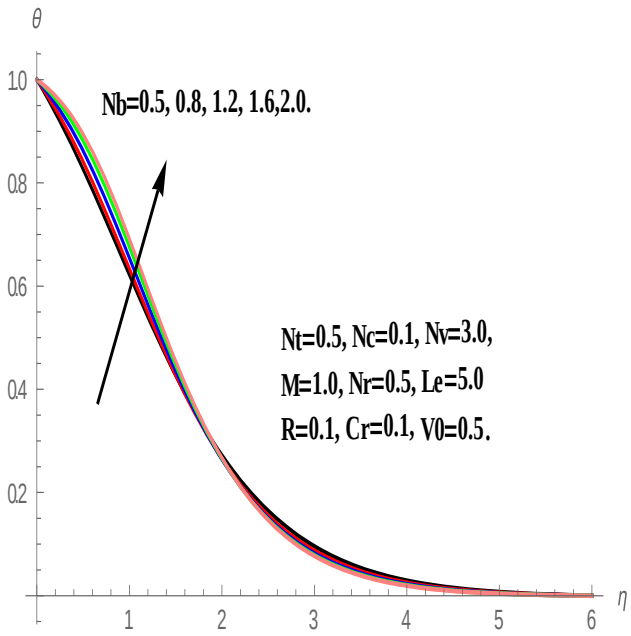

Figure 14.Temperature profiles for various values of (*Nb*)

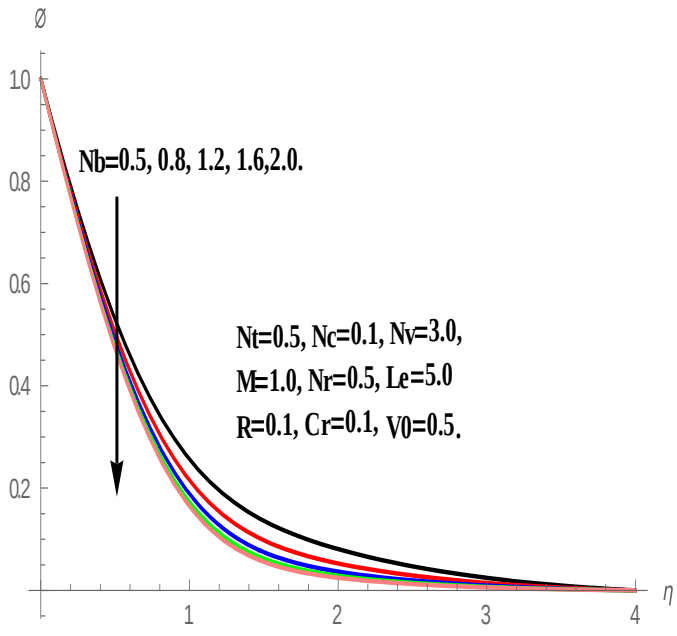

Figure 15.Concentration profiles for various values of (*Nb*)

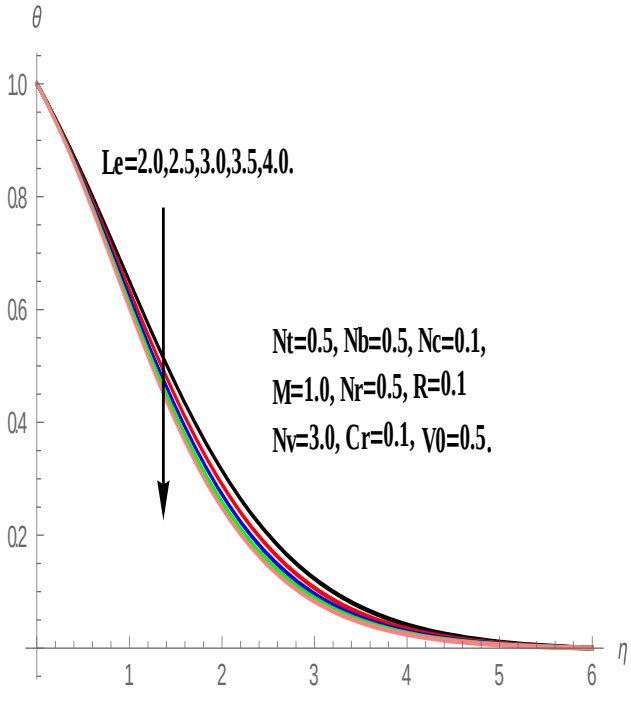

Figure 16.Temperature profiles for various values of (*Le*)

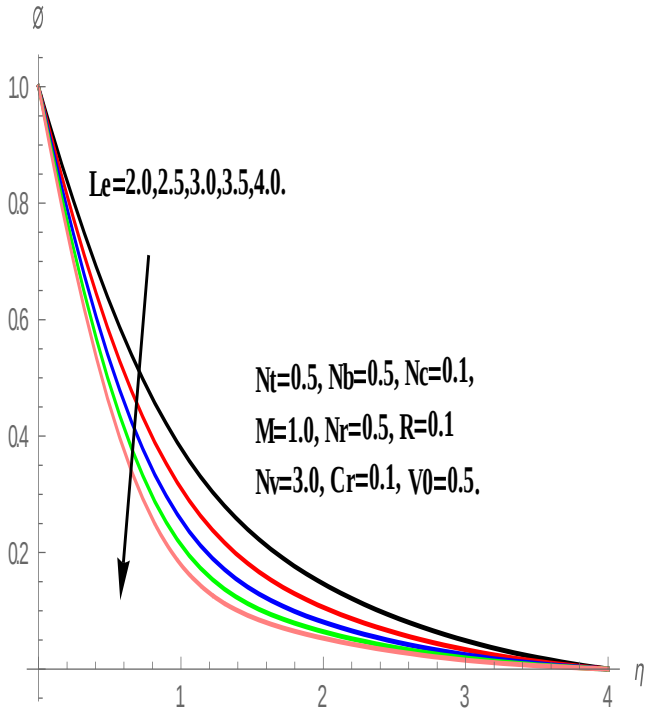

Figure 17.Concentration profiles for various values of (*Le*)

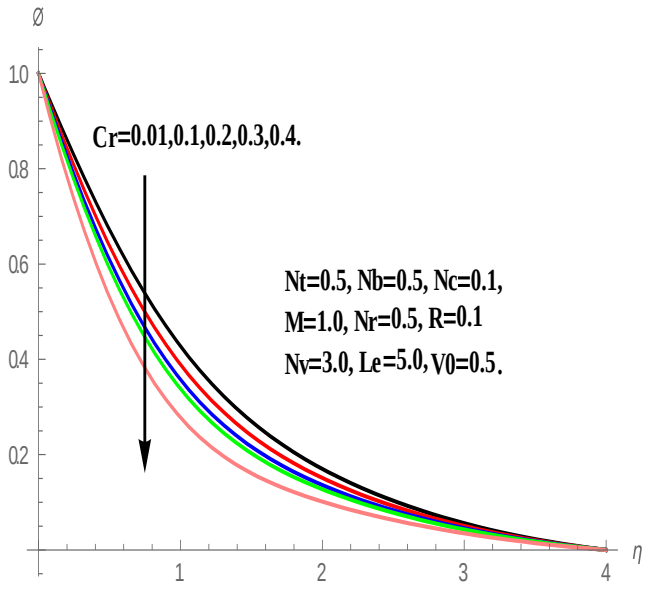

Figure 18.Temperature profiles for various values of (*Cr*)

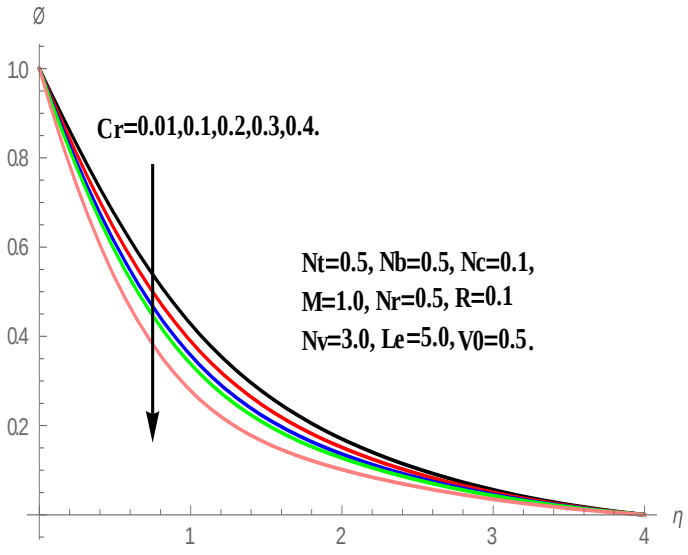

Figure 19.Concentration profiles for various values of (*Cr*)

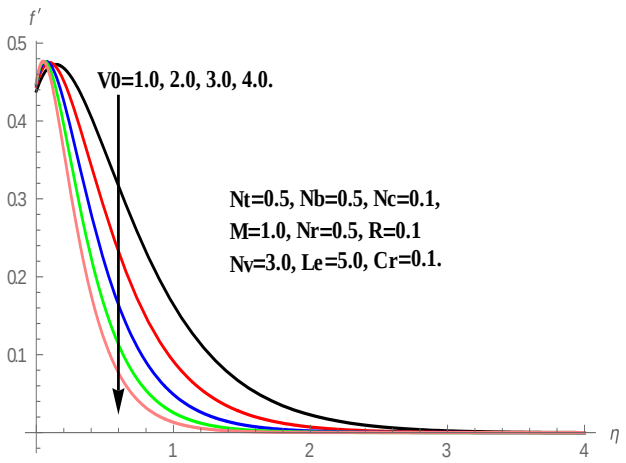

Figure 20.Velocity profiles for various values of (V0)

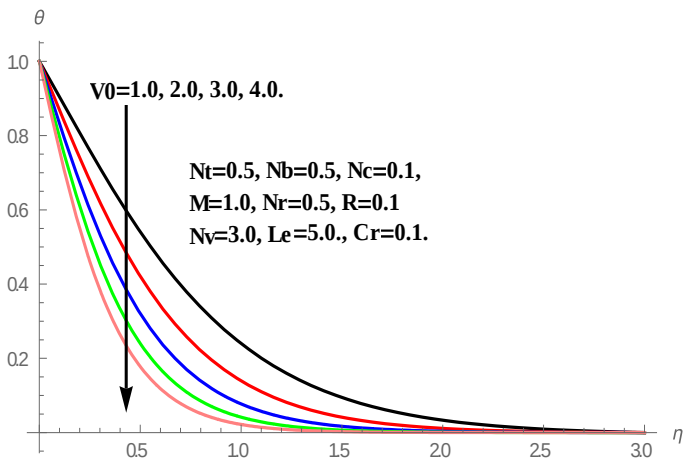

Figure 21.Temperature profiles for various values of (*V0*)

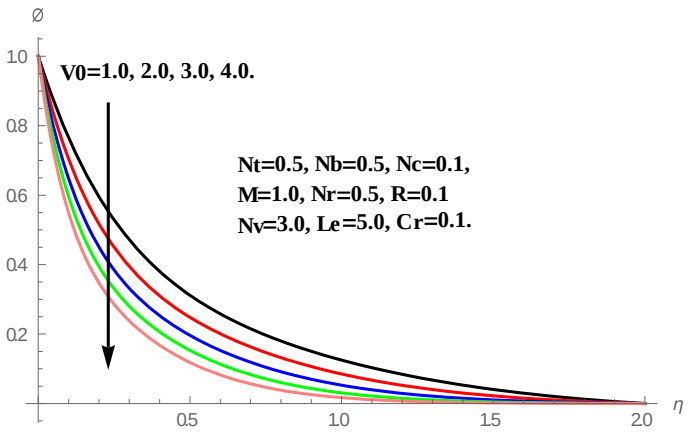

Figure 22.Concentration profiles for various values of (*V0*)

Table 1. Comparison of $-\theta'(0)$ with previously published work with fixed values of $Nt = 10^{-6}, Nb = 10^{-5}, Nr = 10^{-3}, Nc = 0.$

Parameter		Noghrehabadi et al. [30]	Present Study
Nv	*Le*	$-\theta'(0)$	$-\theta'(0)$
2.0	1000	0.7584	0.7591
10.0	1000	0.7670	0.7675
20.0	1000	0.7680	0.7686
200.0	1000	0.7688	0.7694

Table 2. The values of skin – friction coefficient $(-f''(0))$, Nusselt number $(-\theta'(0))$ and Sherwood number $(-\phi'(0))$ for different values of *M, Nr.*

M	Nr	$-f''(0)$	$-\theta'(0)$	$-\emptyset'(0)$
0.5	0.5	0.27975	0.324188	1.10187
1.0	0.5	0.249463	0.313384	1.07352
1.5	0.5	0.214264	0.300098	1.03898
2.0	0.5	0.181968	0.287081	1.00549
2.5	0.5	0.152507	0.274365	0.97311
1.0	0.1	0.563981	0.393473	1.29967
1.0	0.3	0.44246	0.364512	1.21758
1.0	0.5	0.314043	0.331328	1.12398
1.0	0.7	0.184469	0.294269	1.01986
1.0	1.0	0.118862	0.27366	0.96203

Table 3. The values of skin – friction coefficient $(-f''(0))$, Nusselt number $(-\theta'(0))$ and Sherwood number $(-\phi'(0))$ for different values of *Nv, Nc*

Nv	Nc	$-f''(0)$	$-\theta'(0)$	$-\emptyset'(0)$
2.0	0.1	0.111549	0.250542	0.95459
10	0.1	0.191771	0.280877	1.04625
50	0.1	0.249584	0.298977	1.10267
100	0.1	0.321684	0.318761	1.16558
200	0.1	0.363009	0.329025	1.19884
3.0	0.1	0.249584	0.298977	1.10262
3.0	0.5	0.246957	0.260773	1.14362
3.0	1.0	0.244268	0.227302	1.17805
3.0	1.5	0.242007	0.202979	1.20192
3.0	2.0	0.240043	0.184296	1.21945

Table 4. The values of skin – friction coefficient $(-f''(0))$, Nusselt number $(-\theta'(0))$ and Sherwood number $(-\phi'(0))$ for different values of R.

R	$-f''(0)$	$-\theta'(0)$	$-\emptyset'(0)$
0.1	0.249584	0.298977	1.10263
0.3	0.244841	0.297413	1.09859
0.5	0.240635	0.294413	1.09595
0.7	0.236874	0.29085	1.09414
1.0	0.231913	0.284924	1.09234

Table 5. The values of skin – friction coefficient $(-f''(0))$, Nusselt number $(-\theta'(0))$ and Sherwood number $(-\phi'(0))$ for different values of *Nb, Nt.*

Nb	Nt	$-f''(0)$	$-\theta'(0)$	$-\emptyset'(0)$
0.5	0.5	0.249584	0.298977	1.10266
0.8	0.5	0.248543	0.253958	1.14912
1.2	0.5	0.246468	0.19969	1.17792
1.6	0.5	0.244371	0.154741	1.19386
2.0	0.5	0.242879	0.126885	1.20189
0.5	0.1	0.257003	0.38152	1.10534
0.5	0.2	0.255097	0.35994	1.08701
0.5	0.3	0.252839	0.338797	1.07616
0.5	0.4	0.250347	0.319464	1.07305
0.5	0.5	0.249463	0.313384	1.07352

Table 6. The values of skin – friction coefficient $(-f''(0))$, Nusselt number $(-\theta'(0))$ and Sherwood number $(-\phi'(0))$ for different values of Le, Cr.

Le	Cr	$-f''(0)$	$-\theta'(0)$	$-\emptyset'(0)$
2.0	0.1	0.245253	0.289212	0.846374
2.5	0.1	0.248116	0.295031	0.981078
3.	0.1	0.249584	0.298977	1.1026
3.5	0.1	0.250492	0.301924	1.21367
4.0	0.1	0.25113	0.304254	1.31636
5.0	0.01	0.244726	0.285575	0.713854
5.0	0.1	0.245155	0.288495	0.818698
5.0	0.2	0.245462	0.290829	0.911961
5.0	0.3	0.245627	0.292239	0.97314
5.0	0.4	0.246002	0.296484	1.18584

CONCLUSIONS

Impact of variable properties on natural convection boundary layer flow, heat and mass transfer characteristics over a vertical cone embedded in a porous medium saturated by a nanofluid with thermal radiation and chemical reaction is investigated in this research. The important findings of the present study are summarized as follows.

i) The velocity distributions are heightens whereas temperature and nanoparticle volume fraction concentration profiles decelerate in the boundary layer region as the values of variable viscosity parameter (*Nv*) increases.

ii) Increasing values of variable thermal conductivity parameter (*Nc*) elevates the thickness of thermal boundary layer. However, solutal boundary layer thickness deteriorates with the rising values of (*Nc*).

iii) Increasing the values of variable viscosity parameter (*Nv*) rises the dimensionless rates of heat and mass transfer.

iv) As the values of variable thermal conductivity parameter (*Nc*) increases the local Nusselt number values decreases whereas the values of local Sherwood number escalates in the fluid region.

v) Both the temperature and concentration profiles elevates in the boundary layer regime as the values of (*Nt*) increases.

REFERENCES

[1] Choi SUS.,1995 Enhancing thermal conductivity of fluids with nanoparticles, developments and applications of non-Newtonian flows, in: D.A. Siginer, H.P. Wang (Eds.), FED-Vol. 231/MD, Vol. 66, The American Society of Mechanical Engineers pp. 99–105.

[2] Eastman JA, Choi SUS, Li S, Thompson LJ, Lee S. Enhanced thermal conductivity through the development of nanofluid, in: S. Komarneni, J.C. Parker, H.J. Wollenberger (Eds.)., 1997 Nanophase and Nanocomposite Materials II, MRS, Pittsburg, PA pp.3–11.

[3] Eastman JA, Choi SUS, Li S, Yu W, Thompson LJ.,2001 Anomalously increased effective thermal conductivities of ethylene glycol-based nano-fluids containing copper nano-particles. Appl. Phys. Lett. 78 pp.718–720.

[4] Xuan Y, Li Q., 2003 Investigation on Convective Heat Transfer and Flow Features of Nanofluids, ASME J. Heat Transfer, 125 pp.151–155.

[5] Buongiorno J.,2006 Convective transport in nanofluids. ASME J. Heat Transfer 128 pp.240– 250.

[6] Kuznetsov AV, Nield DA.,2010 Natural convection boundary-layer of a nanofluid past a vertical plate. Int. J. Therm. Sci 49 pp. 243–247.

[7] Chamkha. A.J, Rashad. A.M.,2014 Unsteady Heat and Mass Transfer by MHD Mixed Convection Flow from a Rotating Vertical Cone with Chemical Reaction and Soret and Dufour Effects. The Canadian Journal of Chemical Engineering 92 pp.758-767.

[8] Gorla. R.S.R, Chamkha. A.J, Ghodeswar.V.,2014 Natural convective boundary layer flow over a vertical cone embedded in a porous medium saturated with a nanofluid, Journal of Nanofluids 3 pp.65-71.

[9] Behseresht. A, Nogrehabadi. A, Ghalambaz.M., 2014 Natural-convection heat and mass transfer from a vertical cone in porous media filled with nanofluids using practical ranges of nanofluids thermo-physical properties, Chem. Engnrg. Res. Design 92 pp.447-452.

[10] Ghalambaz. M, Behseresht. A, Behseresht. A, Chamkha. A.J, 2015 Effect of nanoparticle diameter and concentration on natural convection in Al_2O_3 -water nanofluids considering variable thermal conductivity around a vertical cone in porous media, Adv. Powder Technology 26 pp.224-235.

[11] Noghrehabadi. A, Behseresht. A, Ghalambaz. M, 2013 Natural convection of nanofluid over vertical plate embedded in porous medium: prescribed surface heat flux, Applied Mathematics and Mechanics 34 pp.669-686.

[12] Noghrehabadi. A, Pourrajab. R, Ghalambaz. M., 2013 Effect of partial slip boundary condition on the flow and heat transfer of nanofluids past stretching sheet prescribed constant wall temperature, International Journal of Thermal Sciences 54 pp.253-261.

[13] Noghrehabadi. A, Saffarian. M. R, Pourrajab. R, Ghalambaz. M., 2013 Entropy analysis for nanofluid flow over a stretching sheet in the presence of heat generation/absorption and partial slip, Journal of Mechanical Science and Technology 27 pp. 927-937.

[14] Teamah. M. A, El-Maghlany. W. M, 2012 Augmentation of natural convection heat transfer in square cavity by utilizing nanofluids in the presences of magnetic field and heat source, International Journal of Thermal Sciences 58 pp.130-142.

[15] Sudarsana Reddy. P, Suryanarayana Rao. K. V, 2015 MHD natural convection heat and mass transfer of Al_2O_3 - water and Ag - water nanofluids over a vertical cone with chemical reaction, Procedia Engineering 127 pp.476 – 484.

[16] Sheremet. M.A., and Pop, I., 2014 Conjugate natural convection in a square porous cavity filled by a nanofluid using Buongiorno's mathematical model, Int. J. Heat Mass Transfer, Vol. 79, pp.137-145.

[17] Sheremet, M.A., Pop, I., and Rahman, M.M.,2015 Three-dimensional natural convection in a porous enclosure filled with a nanofluid using Buongiorno's mathematical model, Int. J. Heat Mass Transfer, vol. 82, pp.396-405.

[18] Ellahi, R., Aziz, S., and Zeeshan, A., 2013 Non

Newtonian nanofluids flow through a porous medium between two coaxial cylinders with heat transfer and variable viscosity, Journal of Porous Media, Vol. **16 (3)**, pp.205-216.

[19] Sheikholeslami, M., Ellahi, R., Mohsan Hassan., and Soheil Soleimani., 2014 A study of natural convection heat transfer in a nanofluid filled enclosure with elliptic inner cylinder, International Journal of Numerical Methods for Heat & Fluid Flow, Vol. 24, pp.1906 – 1927.

[20] Chaim TC., 1996 Heat transfer with variable thermal conductivity in a stagnation point flow towards a stretching sheet. Int Commun Heat Mass Transfer 23, pp.239–248.

[21] Oztop HF, Abu-Nada E., 2008 Numerical study of natural convection in partially heated rectangular enclosures filled with nanofluids. Int J Heat Mass Transfer 29, pp.1326–1336.

[22] Das SK, Choi SUS, Yu W, Pradeep T. 2007 Nanofluids – science and technology. Hoboken: John Wiley & Sons Publishers;.

[23] Chandrasekar M, Suresh S., 2009 A review on the mechanisms of heat transport in nanofluids. Heat Transfer Eng 30 pp.1136–1150.

[24] Khanafer K, Vafai K., 2011 A critical synthesis of thermophysical characteristics of nanofluids. Int J Heat Mass Transfer 54 pp.4410–28.

[25] Kakaç S, Pramuanjaroenkij A., 2009 Review of convective heat transfer enhancement with nanofluids. Int J Heat Mass Transfer 52 pp.3187–3196.

[26] Noghrehabadi. A, Behseresht. A, 2013 Flow and heat transfer affected by variable properties of nanofluids in natural-convection over a vertical cone in porous media, Comput. Fluids 88 pp.313–325

[27] P. Sudarsana Reddy, Ali J. Chamkha, 2016 Influence of size, shape, type of nanoparticles, type and temperature of the base fluid on natural convection MHD of nanofluids, Alexandria Eng. J., 55 pp.331-341.

[28] Anwar Bég, O., Takhar, H. S., Bhargava, R., Rawat, S., and Prasad, V.R., 2008 Numerical study of heat transfer of a third grade viscoelastic fluid in non-Darcian porous media with thermophysical effects, Phys. Scr., 77 pp.1–11.

[29] Sudarsana Reddy, P and Chamkha, AJ, 2016 Soret and Dufour effects on MHD heat and mass transfer flow of a micropolar fluid with thermophoresis particle deposition, Journal of Naval Architechure and Marine Engineering, 13 pp.39-50.

[30] Rana, P., and Bhargava, R., 2012 Flow and heat transfer of a nanofluid over a nonlinearly stretching sheet: a numerical study, Comm. Nonlinear Sci. Numer. Simulat.,17 pp.212–226.

[31] Sudarsana Reddy, P and Chamkha, A.J., 2016 Soret and Dufour effects on MHD convective flow of Al_2O_3–water and TiO_2–water nanofluids past a stretching sheet in porous media with heat generation/absorption, Advanced Powder Technology 27 pp.1207 – 1218.